CBX 98 - $e^{i\pi}$
Harry Nelson
April 13, 1998

On the Resolution in δM

Abstract

This note is about CLEO's resolution in δM.

1 Motivation

A number of physics results would benefit if substantial improvements were made in CLEO's resolution to the the quantity δM, which is loosely the difference between reconstructed and expected D^{*+} masses. Three that come easily to mind are:

- Characterization of $\overline{B^0} \to D^{*+}\ell^-\overline{\nu}$ at high q^2 where the D^{*+} is soft and consequently the background is high.
- Limits on the intrinsic width of the D^{*+}.
- Characterization of 'wrong sign D^0' decays, where backgrounds are high for non-$K\pi$ final states with potentially large branching ratios, such as $D^0 \to K^+\pi^-\pi^0$.

We recognized in 1991 when we proposed the silicon vertex detector (SVX) for CLEO that this device would enable a substantial improvement in CLEO's resolution in δM. We have already achieved much of the promised improvement, as shown in Fig 1, where the resolution is a factor of 3 lower than in the published CLEO-II data[1], a factor of 2 lower than that reported in the re-processing of the CLEO-II data (the 're-compress')[2], which is shown in Fig. 2, and a factor of 2.5-3 lower that proposed for CLEO-III[3] shown in Fig. 3.

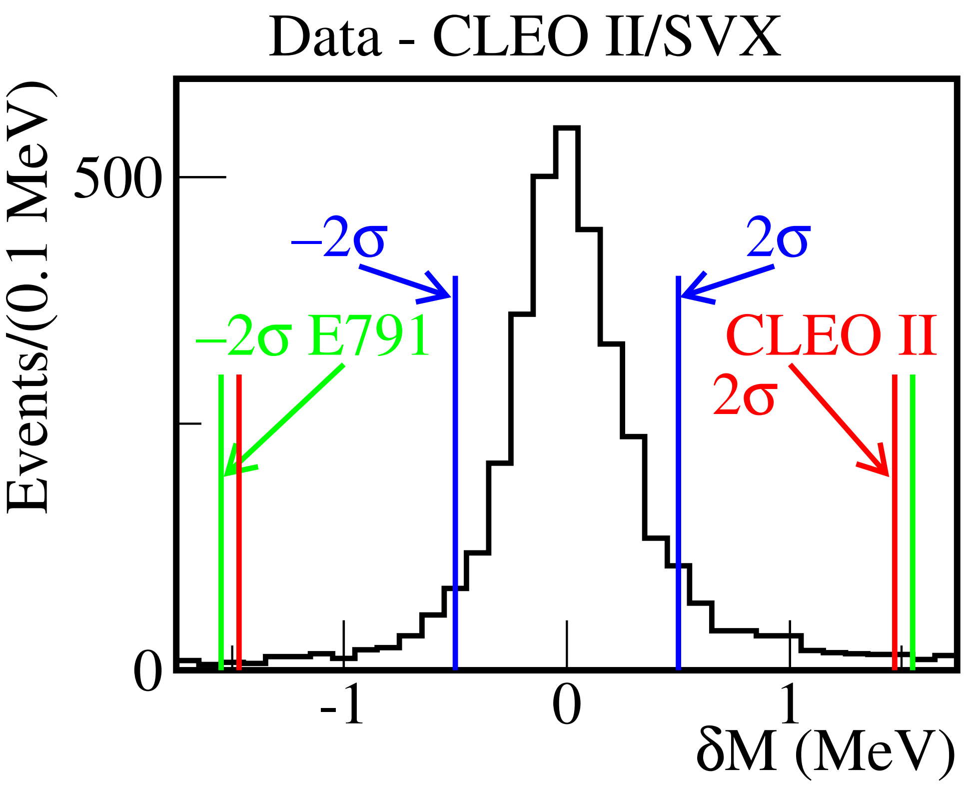

Figure 1: Reconstructed δM from CLEO-II data with the SVX. The central peak has a σ of 250 KeV; subsequent improvements have reduced this σ to 200 KeV. Also shown are the 2σ regions for CLEO-II/SVX, CLEO-II (prior to the re-compress)[1], and for the Fermilab experiment E791[4] are shown. The quantity $\delta M = M_{K\pi\pi} - M_{K\pi} - 145.42\,\mathrm{MeV}$, where the $K^{\mp}\pi^{\pm}$ system has a mass consistent with decay from the D^0, and the momentum of the $K^{\mp}\pi^{\pm}\pi^{\mp}$ system exceeds 2.0 GeV for the CLEO-II/SVX data, and 3.1 GeV for CLEO-II.

The mechanism by which CLEO-II/SVX achieves substantial improvements in δM resolution involves improved measurement of the slow pion from the transition $D^{*+} \to D^0\pi^+$. Indeed, we will make the *approximation* that the resolution in δM is *exclusively caused* by errors in the measurement of the slow pion. On average, this approximation will be accurate because

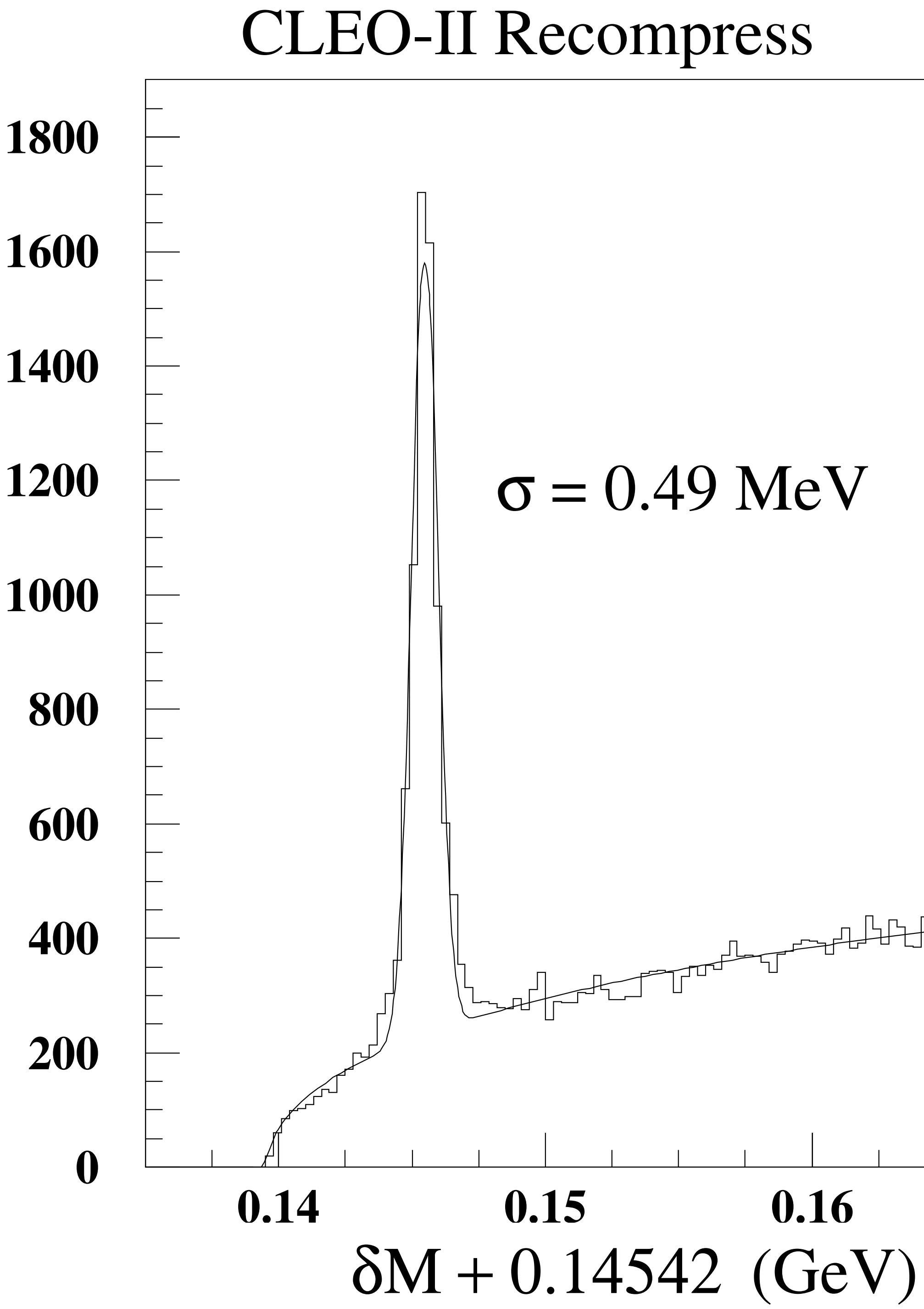

Figure 2: Reconstructed δM from the reprocessed CLEO-II data.

the D^0 decay products are much faster than the slow pion, and therefore the D^0 momentum vector will be reconstructed more accurately than that of the slow pion. There are liable to be particular kinematic configurations of the D^{*+} decay sequence for which errors in the measurement of the D^0 do dominate the resolution in δM, however.

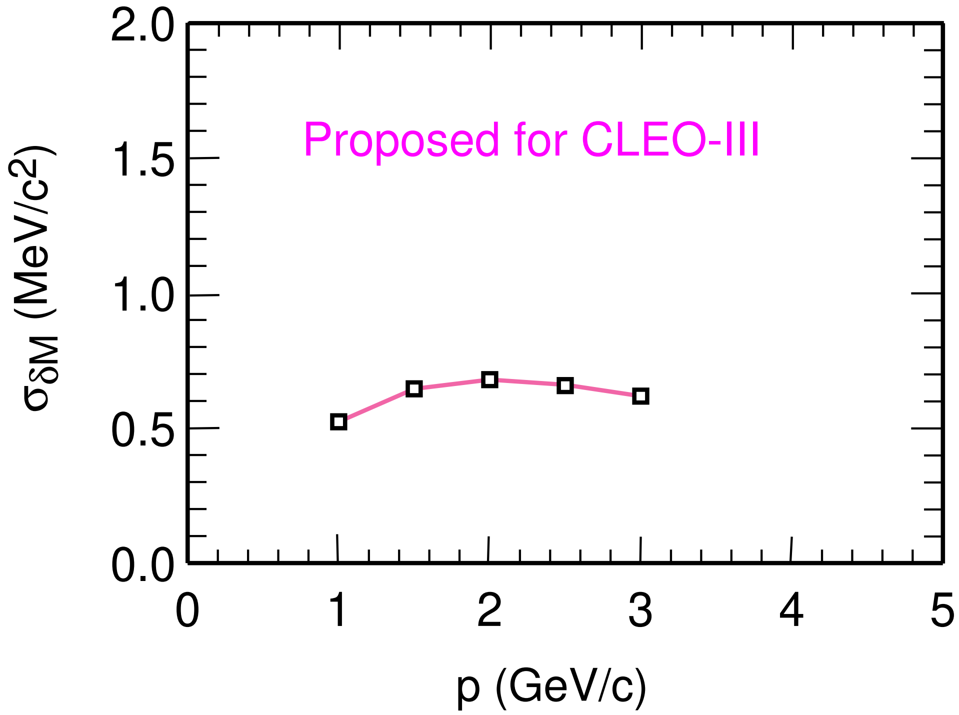

Figure 3: Reconstructed δM proposed for CLEO-III, along the vertical, as a function of the momentum of the D^{*+}, p, along the horizontal.

In the CLEO-II/SVX data, both the angle of the slow pion's trajectory with respect to the e^+ direction, θ_π, and the slow pion's transverse momentum, $p_{t\pi}$, can be measured with substantially greater precision than was possible in earlier data. The improvement in θ_π comes from the 'vertex constrained fit,' which entails in operation:

1. Formation of an estimate for the primary production point of the D^{*+}. Prior to installation of the SVX, the precision on estimation of the

z component of this point was somewhere between 300 and 700 μm. After installation of the SVX, the z component can be estimated with an accuracy of 40 μm.

2. Constraint of the slow pion trajectory to pass through the D^{*+} production point. After installation of the SVX, the first z measurement, made with an accuracy of $27/\sin\theta\,\mu$m, occurs at a radius only 0.35 cm outside the beam-pipe at 2 cm, so a scatter in the beam pipe develops into very little translation where the slow pion penetrates the first layer of the silicon. A constrained fit to the pion trajectory will achieve an accuracy in theta little worse than $\sqrt{40^2+27^2}/23.5 = 2\,\mathrm{mr}$, which at a momentum $p = 100\,\mathrm{MeV}$ is small compared to the multiple scattering in the $(x/X_0) = 0.5\%$ of a radiation length of material in the beam pipe, which is $\approx (15\,\mathrm{mr}/p)\sqrt{x/X_0} = 11\,\mathrm{mr}$.

For the slow pion, it is multiple scattering in the drift chamber itself that dominates the resolution of CLEO in the measurement of $p_{t\pi}$. A gas mixture of 60% Helium, 40% Propane was placed in the CLEO Drift Chamber at the same time the SVX was installed. This gas has a radiation length about three times as long (in meters) as the previous mixture of 50% Argon, 50% Ethane. As a result, the transverse momentum of the slow pion can be measured with substantially better precision in CLEO-II/SVX than in previous CLEO data.

In this note, we estimate the reduction in δM resolution that can be expected from the improvements in the CLEO-II/SVX detector. In principle, the CLEO `GEANT`-based Monte Carlo `CLEOG`, as well as the actual CLEO reconstruction code should be used to make these estimates. However, the CLEO Monte Carlo generation and particularly the track reconstruction are unreliable: the track-fit weight and covariance matrices are still problematic nearly twenty years after CLEO turned on. So, we have opted instead to use a small Monte Carlo to make estimates of resolution in δM.

We do not regard these estimates as definitive, but instead intend them to be useful as a driving force to repair CLEO's track fitting and Monte Carlo generation.

2 Qualitative Argument

The typical resolutions for δM are measured in fractions of an MeV. The typical resolutions for many other mass plots in CLEO are measured in many MeV (for example, see page 56 of reference [3], where the mass resolution for unconstrained $D^0 \rightarrow K^-\pi^+$ is about 6 MeV, and that for unconstrained $\overline{B^0}! \rightarrow \pi^+\pi^-$ is about 20 MeV).

Why?

One explanation, due to Jeff Gronberg, describes the resolution in δM as a consequence of the small $Q = M_{D^{*+}} - M_{D^0} - M_{\pi^+}$ of the D^{*+} decay.

First, assume that misreconstructions of M_{D^0} from its decay products don't matter. In essence, this is true enough, because we when we reconstruct a decay sequence like $D^{*+} \rightarrow D^0\pi^+$, $D^0 \rightarrow K^-\pi^+$, we actually define:

$$\delta M = M_{K\pi\pi} - M_{K\pi} - 145.42\,\text{MeV}; \tag{1}$$

so, knowledge of M_{D^0} really doesn't enter.

If $Q = 0$, then the system of D^0 decay products and the slow π^+ would be **at rest** in the D^{*+} frame, and would therefore, in absence of multiple scattering and inadequacies of measurement in CLEO, appear **collinear** and with the **same speed** when reconstructed.

Perturbations and mismeasurements will cause the D^0 decay products and/or the slow π^+ to seem non-collinear and/or with different speeds.

From such perturbations and mismeasurements, we would infer that back in the rest frame of the D^0 decay products and the slow π^+, they had some relative motion: or that $Q > 0$; and so we would infer that the mass of the decaying state could only be *greater than* the combined mass of the D^0 decay products and the slow π^+. Thus, $\delta M > 0$, and never $\delta M < 0$, and so when $Q = 0$, there is an extremum in the δM as a function of reconstructed quantities. The first derivatives of δM with respect to quantities like θ_π and $p_{t\pi}$ are zero, with the consequence that the reconstructed δM would be very narrow.

For real $D^{*+} \rightarrow D^0\pi^+$ decays, $Q \approx 5.8$ MeV, which is still close enough to zero for the first derivatives of δM with respect to reconstructed quantities to be small. However, in measured in terms of CLEO's experimental resolutions, this Q is sufficiently large that linearizing the dependence of δM on the measured quantities is useful.

3 Derivatives

It is straightforward to work out the derivatives of δM with respect to the two most poorly measured reconstructed quantities of the slow pion, θ_π and $p_{t\pi}$:

$$\frac{\partial(\delta M)}{\partial\theta_\pi} = -\frac{E_{D^0}|\vec{p}_\pi|}{M_{D^{*+}}\sin\theta_\pi}(\beta_\pi\cos\theta_\pi - \beta_{D^0}\cos\theta_{D^0}) \tag{2}$$

$$\frac{\partial(\delta M)}{\partial p_{t\pi}} = \frac{E_{D^0}}{M_{D^{*+}}\sin\theta_\pi}(\beta_\pi - \beta_{D^0}\cos\alpha) \tag{3}$$

where E_{D^0}, β_{D^0}, and θ_{D^0} all refer to quantities that describe the D^0 decay product system in the lab, and $\vec{p}_\pi$, β_π, and θ_π, describe the slow pion in the lab. The angle α is the angle in the lab between the D^0 decay product system direction and the slow pion direction.

If the Q of the $D^{*+}\to D^0\pi^+$ decay vanished, both Eqns. 2 and 3 would vanish as well, because the speeds in the lab of the slow pion and the system of D^0 decay products would be the same ($\beta_\pi = \beta_{D^0}$) and the two would be collinear in the lab: $\cos\alpha = 1$ and $\cos\theta_\pi = \cos\theta_{D^0}$. This is a more precise version of the qualitative argument made in the last section.

When the Q of the $D^{*+}\to D^0\pi^+$ decay is non-zero, as really happens in Nature, it *still* can happen that one or both of Eqns. 2 and 3 may vanish. Indeed, the fact that neither Eqn. 2 nor Eqn. 3 is constant across the kinematics of the decay means that the measurement errors in θ_π and $p_{t\pi}$ will be amplified or suppressed considerably, depending on the kinematics of the decay. As a result, the δM peak will not be a single Gaussian, but will be a superposition of a spectrum of Gaussians. This tendency is more pronounced in the data taken before the installation of the SVX, and has necessitated the use of *at least* double Gaussian when a fit is made to the δM distribution.

4 Error in θ_π: σ_θ

We make the approximation that the error in θ_π results alone from the error in z on the primary D^{*+} production point or vertex, the error on the first measurement of z in the tracking system, and multiple scattering in the beam pipe. Additional information from subsequent tracking layers can in principle help determine θ_π, but in the limit of a very soft pion, the improvement in the determination of θ by the additional tracking layers vanishes.

The situation is described in Fig. 4. The primary production point or vertex of the D^{*+} is determined with an error in z of σ_{vz}, in general through a combination of a variety of information, including the location and size of the e^+e^- annihilation region, the direction and trajectory of the D^0 decay product system, and tracks that are not associated with the D^{*+}. The slow pion from the $D^{*+} \to D^0\pi^+$ makes an angle θ_π with the beam axis, and proceeds to the beam pipe of thickness X in radiation lengths at the radius r_{bp}, where the pion scatters by the amount $\delta\theta$ in polar angle, and:

$$\delta\theta = \frac{13.6 \text{ mr}}{\beta_\pi|\vec{p}_\pi|(\text{GeV})}\sqrt{\frac{X}{\sin\theta_\pi}}\left[1 + 0.038\ln\left(\frac{X}{\sin\theta_\pi}\right)\right]. \tag{4}$$

The slow pion then proceeds a further distance r_g to the tracking layer that makes the first z sample with precision σ_{sz}.

We calculate the error that a reconstruction of θ_π made by simply connecting the primary vertex with the first measurement of z. A true vertex constrained fit must have an error smaller than the error on this simple reconstruction, but the two must converge as $p\to 0$, in which limit the subsequent tracking layers do not help to measure the slow pion. The error on the simple reconstruction, σ_θ, is[5]:

$$\sigma_\theta = \frac{\sqrt{[\sigma_{vz}^2 + \sigma_{sv}^2]\sin^4\theta_\pi + [r_g\delta\theta]^2}}{(r_g + r_{bp})} \tag{5}$$

The various quantities needed for the evaluation of σ_θ, for CLEO-II and CLEO-II/SVX, are given in Tab. 1.

5 Error in $p_{t\pi}$: σ_{p_t}

We make the approximation that the multiple scattering in the drift chamber alone contributes the dominant term to σ_{p_t}. This approximation is appropriate at low momentum, because in essence, multiple scattering in the material in between the inner tracking layers such as the silicon detector, and the drift chamber renders the benefit of combining information from those devices

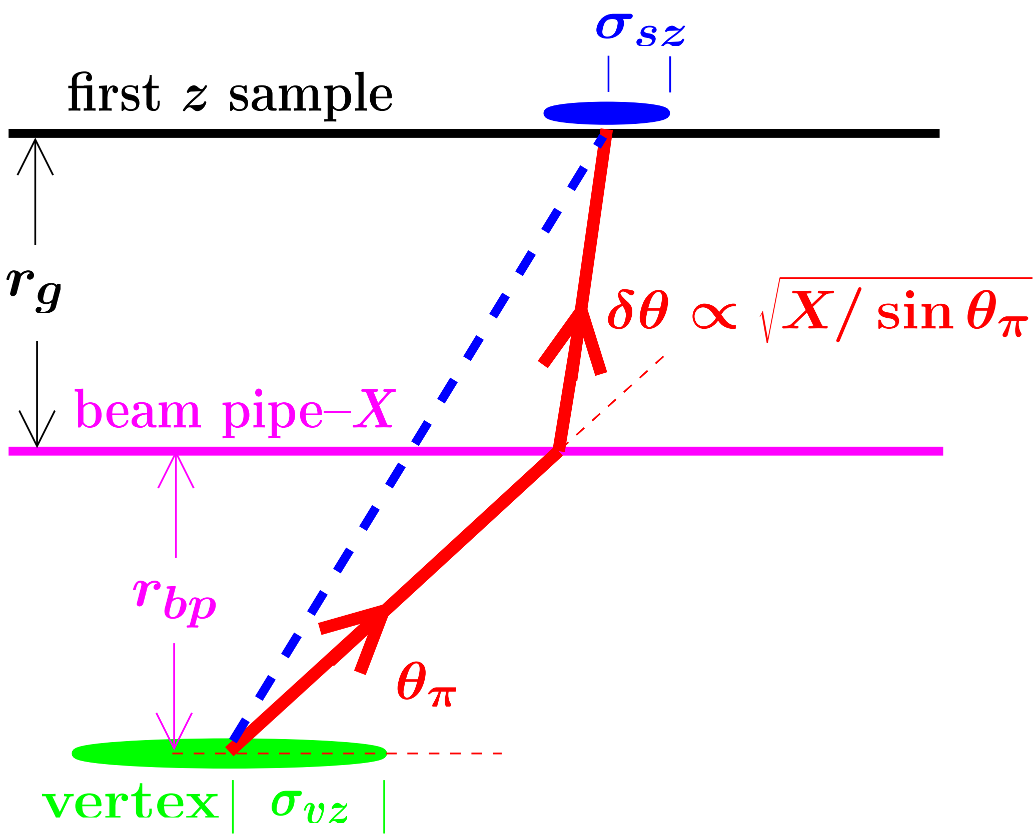

Figure 4: Quantities needed for estimation of the error in θ_π, σ_θ. The primary vertex, where the D^{*+} originated, is measured with an error in z of σ_{vz}, through a combination of a variety of information including the location and size of the e^+e^- annihilation region, the direction and trajectory of the D^0, and the trajectories of tracks that are neither from the slow pion nor the D^0 decay products. The slow pion from the $D^{*+} \to D^0\pi^+$ decay makes an angle θ_π with the beam axis, and proceeds to the beam pipe at a radius of r_{bp}, which has a thickness in radiation lengths of X. The pion scatters by an angle $\delta\theta$ in the beam pipe. The first z sample occurs at a distance of r_g from the beam pipe, and provides a measurement accuracy of σ_{sv}. A vertex constrained fit for θ_π should achieve an error less than reconstruction by simply connecting the primary vertex and the first z sample, which is shown by the dotted line.

Table 1: Values of the variables described in Fig. 4

	CLEO-II	w/SVX	units
σ_{sz}	1200	$27/\sin\theta$	μm
σ_{vz}	300	40	μm
r_g	4.5	0.35	cm
$r_g + r_{bp}$	8.47	2.35	cm
X	0.46	0.51	% r.l.

small. We neglect the straggling in energy lost as the particle penetrates the matter between the interaction point and the drift chamber.

The resolution σ_{p_t} is[6]:

$$\sigma_{p_t} = \left[\frac{0.016}{0.3B\beta_\pi \sin^{3/2}\theta_\pi} \frac{1}{L_\perp} \sqrt{\frac{L_\perp}{X_0}} \right] p_{t\pi} \tag{6}$$

Here, B is the strength of the magnetic field that permeates the drift chamber, in Tesla; $L_\perp$ is the segment of the circle in the $x-y$ projection of the slow pion's track in the drift chamber, in meters; and $L_\perp/X_0$ is the segment measured in radiation lengths of the tracking medium. The segment $L_\perp$ is shown in Fig. 5. The segment $L_\perp$ is a function of the magnetic field B, the inner and outer radii of the drift chamber, $r_i = 19.9\,\mathrm{cm}$ and $r_o = 90.1\,\mathrm{cm}$, and $p_{t\pi}$.

To obtain the relationship between $L_\perp$ and $p_{t\pi}$, it is useful to denote the minimum transverse momentum needed to penetrate to the inner and outer radii of the drift chamber, respectively:

$$p_{ti} = 0.3B\frac{r_i}{2} = 45\,\mathrm{MeV} \tag{7}$$

$$p_{to} = 0.3B\frac{r_i}{2} = 203\,\mathrm{MeV} \tag{8}$$

From Fig. 5, the azimuth of the slow pion about the center of its orbit, upon entrance to the drift chamber, ϕ_i, and the similar angle upon exit from

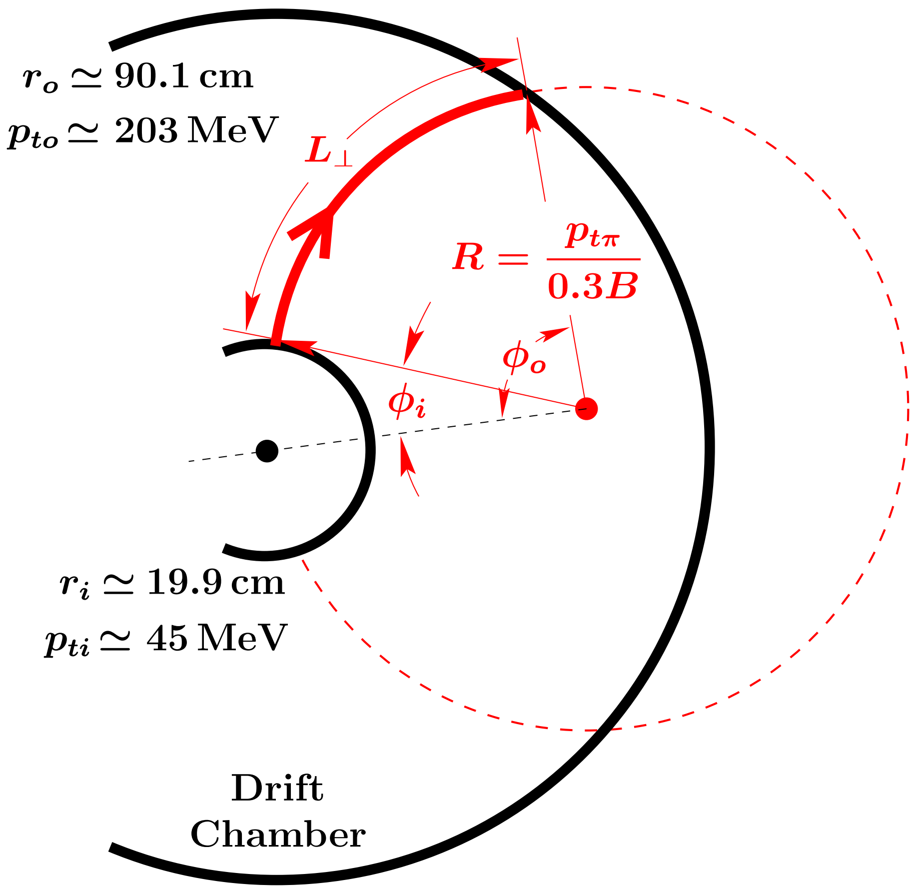

Figure 5: Quantities needed for resolution in reconstruction of $p_{t\pi}$. The slow pion leaves the interaction point at the center of the drift chamber and proceeds on the segment of the circle shown, which has radius $R = p_{t\pi}/(0.3B)$. The quantity $L_\perp$ is the length of the arc measured in the drift chamber; in practice $L_\perp$ includes no more than the first semicircle of the slow pion's orbit. The inner radius of the Drift Chamber, r_i, is 19.9 cm: neglecting energy loss, the transverse momentum of the slow pion $p_{t\pi} > p_{ti} = 45\,\mathrm{MeV}$ to penetrate further than the inner radius; similarly, the transverse momentum of the slow pion $p_{t\pi} > p_{to} = 203\,\mathrm{MeV}$ to penetrate further than the outer layer of the drift chamber. The angle ϕ_i describes the azimuth about the center of the slow pion's circular orbit reached when the slow pion penetrates the first layer of the drift chamber; the angle ϕ_o describes the azimuth about center of the slow pion's circular orbit reached upon exit through the outer wall of the drift chamber.

the drift chamber ϕ_o, are:

$$\begin{aligned} \phi_i &= 2\sin^{-1}\left(\frac{p_{ti}}{p_{t\pi}}\right) & p_{t\pi} > p_{ti} \\ \phi_o &= 2\sin^{-1}\left(\frac{p_{to}}{\max(p_{t\pi}, p_{to})}\right) \end{aligned} \tag{9}$$

In terms of these quantities, the segment $L_\perp$ is:

$$L_\perp = R|\phi_o - \phi_i| \quad \xrightarrow{p_{t\pi}\to\infty} \quad r_o - r_i \tag{10}$$

The quantity $x \equiv 1/X_0$, where then $L_\perp/X_0 = xL_\perp$ depends on the wires and gas in the drift chamber. For CLEO, the wires have always been the same, but the gas was changed from 50% Argon, 50% Ethane to 60% Helium, 40% Propane when the SVX was installed. We summarize the various contributions to x, both before and after the gas change, in Tab. 2.

Table 2: Matter, in radiation lengths/meter, in the drift chamber.

Type	x (% r.l./meter)
Gold on Field Wires	0.25
Aluminum in Field Wires	0.15
Sense Wires	0.03
Total Wires	**0.43**
50% Argon	0.43
50% Ethane	0.15
Gas CLEO-II	0.57
Total CLEO-II	**1.00**
60% Helium	0.01
40% Propane	0.17
Gas CLEO-II/SVX	0.18
Total CLEO-II/SVX	**0.61**

A consequence of the long radiation length of the mixture used in the CLEO-II/SVX drift chamber is that the wires comprise about 70% of the material in the chamber. However, wires are localized, so when a scatter occurs in a wire, a clear kink in the track is often produced. It is conceivable in the CLEO-II/SVX data, to reduce or even eliminate the loss in p_t resolution brought about by scattering in the wires, by searching for and refitting kinks that occur for tracks that pass close, according to the track fit, to a wire.

6 Fast Monte Carlo

We have studied the resolution in δM that results from smearing the slow pi from $D^{\star +} \rightarrow D^0\pi^+$ decay according to Eqns. 5 and 6. We use a fast Monte Carlo simulation to do so.

In the fast Monte Carlo, $2{\times}10^6$ D^{*+} at a single momentum are generated with a $1 + \cos^2\theta$ distribution out to $|\cos\theta = 0.7|$, where θ is respect to the beam line. Then, the decay products of the D^{*+}, the D^0 and the π^+ are assigned a randomly chosen decay axis in the D^{*+} rest frame, and the slow π^+ is boosted to the lab frame. Only slow pions that penetrate to the DR, that is to 19.9 cm from the beam axis, and that fall into the region $|\cos\theta_\pi| < 0.8$ are considered. The effect of dE/dx is neglected. Uncorrelated Gaussian smearing according to Eqns. 5 and 6 are then applied, and then δM is reconstructed. The *root-mean-squared* (rms) δM is computed; and results are shown in Fig. 6.

We have evaluated three scenarios:

1. For CLEO-II, as described in the first column of Tab. 1; a vertex-constrained fit, possible only in the 'recompressed' data is assumed.

2. For CLEO-II/SVX, as described in the second column of Tab. 1.

3. For CLEO-II/SVX, with deletion of the material in the wires in the DR: this is the limit that could be achieved by the fitting of kinks in the track trajectory at the intersection of the trajectory with the wire.

Qualitatively, at low momentum of the D^{*+} the rms of δM is dominated by the resolution in $p_{t\pi}$ described by Eqns. 6 and 3, and at high momentum the contribution in the resolution in θ_π described by Eqns. 5 and 2 dominates.

The distribution in δM is, in general, strongly non-Gaussian. So, the rms differs from the result one would obtain with various types of Gaussian fits. A common strategy in CLEO is to fit peaks with a superposition of two

Gaussians, with normalizations A_1 and A_2, and width parameters σ_1 and σ_2, and then to define:

$$\overline{\sigma}_{\delta M} \equiv \sqrt{\frac{A_1\sigma_1^2 + A_2\sigma_2^2}{A_1 + A_2}}. \tag{11}$$

The results of double Gaussian fits to the same data upon which Fig. 6 is based are shown in Fig. 7.

In general, the quantity $\overline{\sigma}_{\delta M}$ is smaller than the rms in δM, and the difference is most pronounced for the CLEO-II recompress scenario. Indeed, the non-gaussian tails for CLEO-II recompress case are so long that they might end up difficult to discriminate from background.

7 Event-by-event errors

As a cross check within the fast Monte-Carlo, and as a check on the non-Gaussian tails discussed in the previous section, we compute the expected error in the mass the derivative equations, Eqns. 2 and 3 are combined with Eqns. 5 and 6 to yield a prediction for the resolution in δM on an event-by-event basis:

$$\sigma_{\delta M}^2 = \sigma_\theta^2 \left[\frac{\partial(\delta M)}{\partial\theta_\pi}\right]^2 + \sigma_{p_t}^2 \left[\frac{\partial(\delta M)}{\partial p_{t\pi}}\right]^2 .$$

References

[1] D. Cinabro *et. al.*, Phys. Rev. Lett. **72**, 1406 (1994).

[2] CLEO Collaboration, 'Report to the PAC,' CBX 96-102 (Dec. 1996) p. 19.

[3] CLEO Collaboration, 'The CLEO III Detector, Design and Physics Goals,' `URL: http://www.lns.cornell.edu/public/CLEO/-CLEO3/CLEO3.html`, February 18, 1994, Page 55.

[4] E.M.Aitala *et. al.*, Phys. Rev. **D57**, (1998); `hep-ex/9608018`.

[5] Particle Data Group, 'Review of Particle Properties,' Phys. Rev. **D54**, 1 (1996): Section 22.6, Eqn. 22.8, page 134.

[6] Particle Data Group, 'Review of Particle Properties,' Phys. Rev. **D54**, 1 (1996): Section 24.8, Eqn. 24.19, page 147.

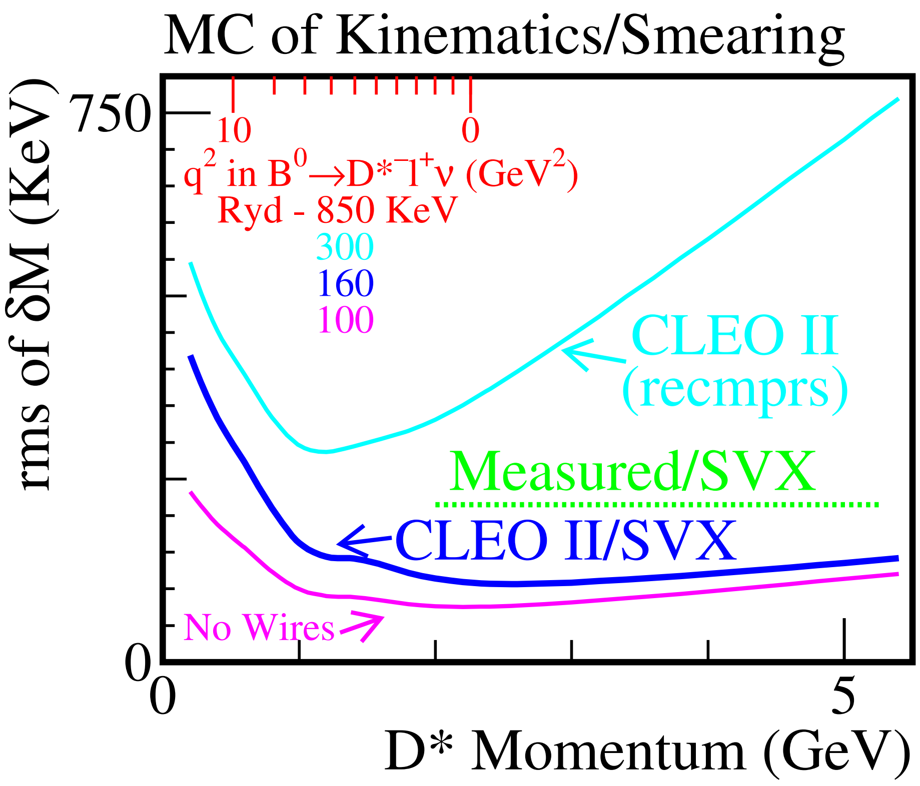

Figure 6: The *root-mean-squared*(rms) δM from the fast Monte Carlo for three scenarios: for CLEO-II and for the CLEO-II/SVX, as described by the parameterization in Table 1. For CLEO-II/SVX, wires make the dominant contribution to multiple scattering in the tracking volume of the Drift Chamber (DR). It may well be possible to suppress the contribution of multiple scattering in the wires to the mismeasurement of transverse momentum by allowing for kinks in tracks that pass near to wires; the lower limit on the rms δM that would result if all influence due to scattering in the wires is shown in the third, lowest curve. Qualitatively, multiple scattering in the DR dominates the rms at small D^{*+} momentum, and mismeasurement of polar angle θ_π dominates the rms at large D^{*+} momentum. For the case of CLEO-II at large D^{*+} momentum, the distribution is very non-Gaussian, so the rms will in general differ from estimates of σ from Gaussian fits. In the upper right curve the scale of the q^2 in $\overline{B^0} \to D^{*+}\ell^-\overline{\nu}$ decay is shown, as well as the resolution in δM obtained in one CLEO result on the form factors involved in that decay, where data prior to the improvement in the error matrices brought about by the recompress was used. The rms evaluated at $q^2 = 8\,\mathrm{GeV}^2$, or a momentum of the D^{*+} of $1\,\mathrm{GeV}$, is also shown for the three scenarios evaluated here.

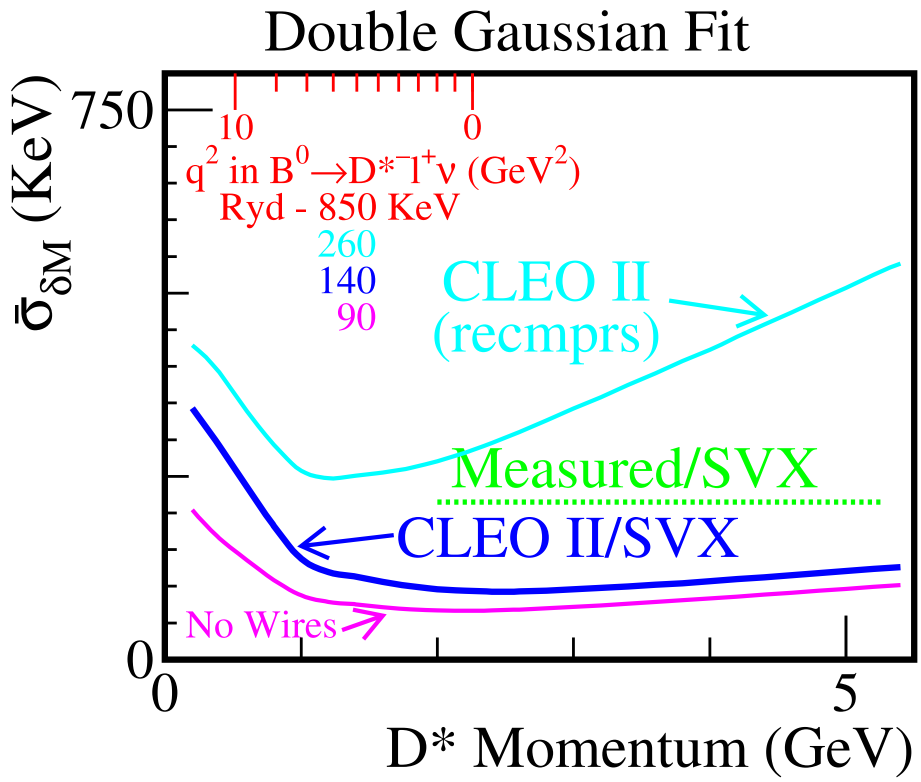

Figure 7: The parameter $\overline{\sigma}_{\delta M}$ as defined in Eqn. 11, for the same data upon which Fig. 6 is based. In general, in all cases the parameter $\overline{\sigma}_{\delta M}$ is smaller than the rms depected in Fig. 6; the fractional difference is largest in the case of the CLEO-II recompress scenario. For more details, see the caption of Fig. 6.